

Rowan University

Rowan Digital Works

Henry M. Rowan College of Engineering
Departmental Research

Henry M. Rowan College of Engineering

5-30-2024

Reconfigurable modular soft robots with modulating stiffness and versatile task capabilities

Joshua Knospler
Rowan University

Wei Xue

Mitja Trkov

Follow this and additional works at: https://rdw.rowan.edu/engineering_facpub



Part of the [Engineering Commons](#)

Recommended Citation

Knospler, Joshua; Xue, Wei; and Trkov, Mitja, "Reconfigurable modular soft robots with modulating stiffness and versatile task capabilities" (2024). *Henry M. Rowan College of Engineering Departmental Research*. 324.

https://rdw.rowan.edu/engineering_facpub/324

This Article is brought to you for free and open access by the Henry M. Rowan College of Engineering at Rowan Digital Works. It has been accepted for inclusion in Henry M. Rowan College of Engineering Departmental Research by an authorized administrator of Rowan Digital Works.

PAPER • OPEN ACCESS

Reconfigurable modular soft robots with modulating stiffness and versatile task capabilities

To cite this article: Joshua Knospler *et al* 2024 *Smart Mater. Struct.* **33** 065040

View the [article online](#) for updates and enhancements.

You may also like

- [Enhanced Oxygen Reduction Using Triode Fuel Cells](#)
Costas G Vayenas, Eftyhia Martino and Alexandros Katsaounis
- [Life Testing of Ni-YSZ Fuel Electrode Under Electrolysis and Fuel Cell Operation in High Reducing Environment](#)
Qinyuan Liu, Qian Zhang, Peter W Voorhees et al.
- [On coherence of quantum operations by using Choi–Jamiokowski isomorphism](#)
Xiaorong Wang, Ting Gao and Fengli Yan



The Electrochemical Society

Advancing solid state & electrochemical science & technology

DISCOVER
how sustainability
intersects with
electrochemistry & solid
state science research



Reconfigurable modular soft robots with modulating stiffness and versatile task capabilities

Joshua Knospler , Wei Xue  and Mitja Trkov* 

Department of Mechanical Engineering, Rowan University, 201 Mullica Hill Rd, Glassboro, NJ 08028, United States of America

E-mail: trkov@rowan.edu

Received 12 December 2023, revised 19 April 2024

Accepted for publication 17 May 2024

Published 30 May 2024



CrossMark

Abstract

Soft robots have revolutionized machine interactions with humans and the environment to enable safe operations. The fixed morphology of these soft robots dictates their mechanical performance, including strength and stiffness, which limits their task range and applications. Proposed here are modular, reconfigurable soft robots with the capabilities of changing their morphology and adjusting their stiffness to perform versatile object handling and planar or spatial operational tasks. The reconfiguration and tunable interconnectivity between the elemental soft, pneumatically driven actuation units is made possible through integrated permanent magnets with coils. The proposed concept of attaching/detaching actuators enables these robots to be easily rearranged in various configurations to change the morphology of the system. While the potential for these actuators allows for arbitrary reconfiguration through parallel or serial connection on their four sides, we demonstrate here a configuration called ManusBot. ManusBot is a hand-like structure with digits and palm capable of individual actuation. The capabilities of this system are demonstrated through specific examples of stiffness modulation, variable payload capacity, and structure forming for enhanced and versatile object manipulation and operations. The proposed modular, soft robotic system with interconnecting capabilities significantly expands the versatility of operational tasks as well as the adaptability of handling objects of various shapes, sizes, and weights using a single system.

Supplementary material for this article is available [online](#)

Keywords: stiffness modulation, grasping, permanent magnets with coils, attachable and detachable actuators, reconfigurations, modular robots, soft robots

1. Introduction

Robotic grasping and object manipulation have been inspired by the remarkable abilities of human hands. Recent advances

in soft robotic actuators, tactile sensors, materials, visual and haptic perception, and machine learning have enabled significant progress toward dexterous human-like robotic grasping [1–3]. Development of soft robots has opened up new possibilities for grasping and functional tasks due to their inherent material and structural compliance properties [4–6]. Despite the recent progress, most of the soft robotic manipulators and grippers are limited to performing dedicated operational tasks. For soft robots to perform versatile, on-demand tasks that would require them to change stiffness, shape, or morphology still presents a challenge. Varying, adapting, and

* Author to whom any correspondence should be addressed.



Original content from this work may be used under the terms of the [Creative Commons Attribution 4.0 licence](#). Any further distribution of this work must maintain attribution to the author(s) and the title of the work, journal citation and DOI.

controlling the deformability and compliance of soft robots remains an open challenge; hence, advancements that would enable selective or variable stiffness of these machines could open up new soft robot functionalities [7]. Some of these challenges can potentially be addressed by developing new modular, self-reconfigurable soft robots with the capabilities to modulate their mechanical properties based on the given task [8, 9]. These modular soft robots can provide significant advantages over traditional systems, such as the overall increased safety when soft robots are working next to humans and the enhanced versatility of tasks performed by modular robots. Using modular designs enables replacing task-specific robots with a single robot, leading to increased productivity and reduced costs for the end users. Further development of these new technologies would enhance the functionality of soft robots, and the adoption of these systems in industrial applications will enable safer and more efficient human-robot interactions [10, 11].

The existing reconfigurable, modular soft robots are commonly constructed from individual, simple, soft material-based modular actuation units and rigid/hard components used for connectivity [8, 9, 12, 13]. Recent developments in the field have witnessed a notable shift towards utilizing 3D printing technology for fabricating modular, soft robots tailored for grasping applications [14, 15]. The sizes of these modular robots can already reach up to a meter-scale [16]. Such soft modular systems have shown to have an increased functionality and an ability to perform various functions (e.g. manipulation, locomotion, or human assistance/rehabilitation) in different environments (e.g. complex terrain, ferromagnetic walls, or underwater) [13, 16–25]. Advantages of shape-changing capabilities have been very recently demonstrated through a shape-changing robot that outperformed the non-morphing counterpart in its abilities to traverse flat and inclined terrains [26]. Furthermore, controllable stiffness modulation has been noted to be of great importance to expand the operational capabilities of soft robots [21, 26, 27]. Inspired by nature, on-demand variable stiffness that allows reversible changes between compliant/flexible and rigid modes has been recently demonstrated through plant inspired (osmosis-based actuated) soft robots [28]. Such variable stiffness modes can then be pre-programmed or tailored for a range of specific tasks through the optimization of the robots' interactions with the environment and their increased capabilities to exert high forces or bear heavy loads [27]. The four basic stiffness modulation mechanisms employed in the existing soft robots are classified as glass/phase transition, viscosity, structure, and acoustic-based methods with none of them clearly outweighing the others. Among them, structural stiffness variation method has primarily focused on either the interactions between structural elements within an individual actuation unit (e.g. employing geometry or friction principles, material jamming, or antagonistic arrangement) or through direct tuning of material rigidity (e.g. material phase change of polymers or low melting point alloys) [29]. However, the morphology reconfiguration of soft, multi-actuator units to vary the structural stiffness at the system level remains largely unexplored.

Despite all the potential advantages and unique capabilities of modular soft robots, currently only very limited soft reconfigurable robots with stiffness modulation capabilities exist. One of the challenges in soft robot reconfigurability is the connectivity between the soft actuation modules which should be simple and fast to connect or disconnect in either controlled or autonomous fashion. Most commonly used connectivity mechanisms rely on mechanical, magnetic, adhesive, and vacuum principles [9]. Among these, the magnetic mechanism is an attractive option as it can actively control the interconnection of modules by using either permanent magnets with predefined magnetic fields [8], electropermanent magnets (EPM) that allow tunable connectivity based on the applied electric current [30], or magnetic soft composites with pre-programmable magnetization [31]. While these magnetic devices have promising potential in modular robotics, their current applications have two major limitations: (1) the non-articulating connection between the units that hinder the structural reconfigurability and stiffness tuning, and (2) the added rigidity to the soft modular unit itself from the embedded hard components. By contrast, other mechanisms such as electro adhesion [32] and vacuum-based connections [33] maintain the softness of the modular robots. However, these systems typically have limited attractive forces or require additional connection modules, restricting their practicality for the autonomous reconfiguration. Lastly, while several other passive connection methods exist, most of them are irreversible as they are either glued [34], hot-melted [35], or connected by self-healing elastomer [36] with only limited devices being reversible, such as reclosable fasteners [37]. However, the passive connections do not allow for control of the connections or the ability to tune its strength due to their inherent passive nature.

Here, we present a new set of soft, modular, and reconfigurable robots (figure 1) that can be assembled to modulate its structural stiffness and perform versatile operational tasks, due to its novel tunable interlocking mechanism. The proposed soft robotic system is constructed of identical elemental soft actuators (figure 1(a)). The permanent magnets with coils (PMC), whose design was inspired by the EPMs [33, 38], are used to interlock the units. Using the modular elemental units, a robot configuration called ManusBot was assembled that consists of two units connected in series via the end magnets with additional units connected to their side magnets, creating a hand-shaped soft robot with a multi-finger actuator configuration. We demonstrate that ManusBot can grasp objects of various shapes and sizes, as well as modulate its stiffness by reconfiguring its finger-like actuators. The functional abilities of this configuration were tested experimentally to determine its effectiveness as a grasping robot. Overall, through testing of the individual actuators and various configurations of planar and closed-form structures we demonstrated enhanced functionalities and stiffness modulation capabilities. Our modular design allows a single robotic system to handle a wide variety of tasks that are typically unattainable using a single robot.

The key novelty and significance of the project are the innovative structural stiffness modulation of modular robots

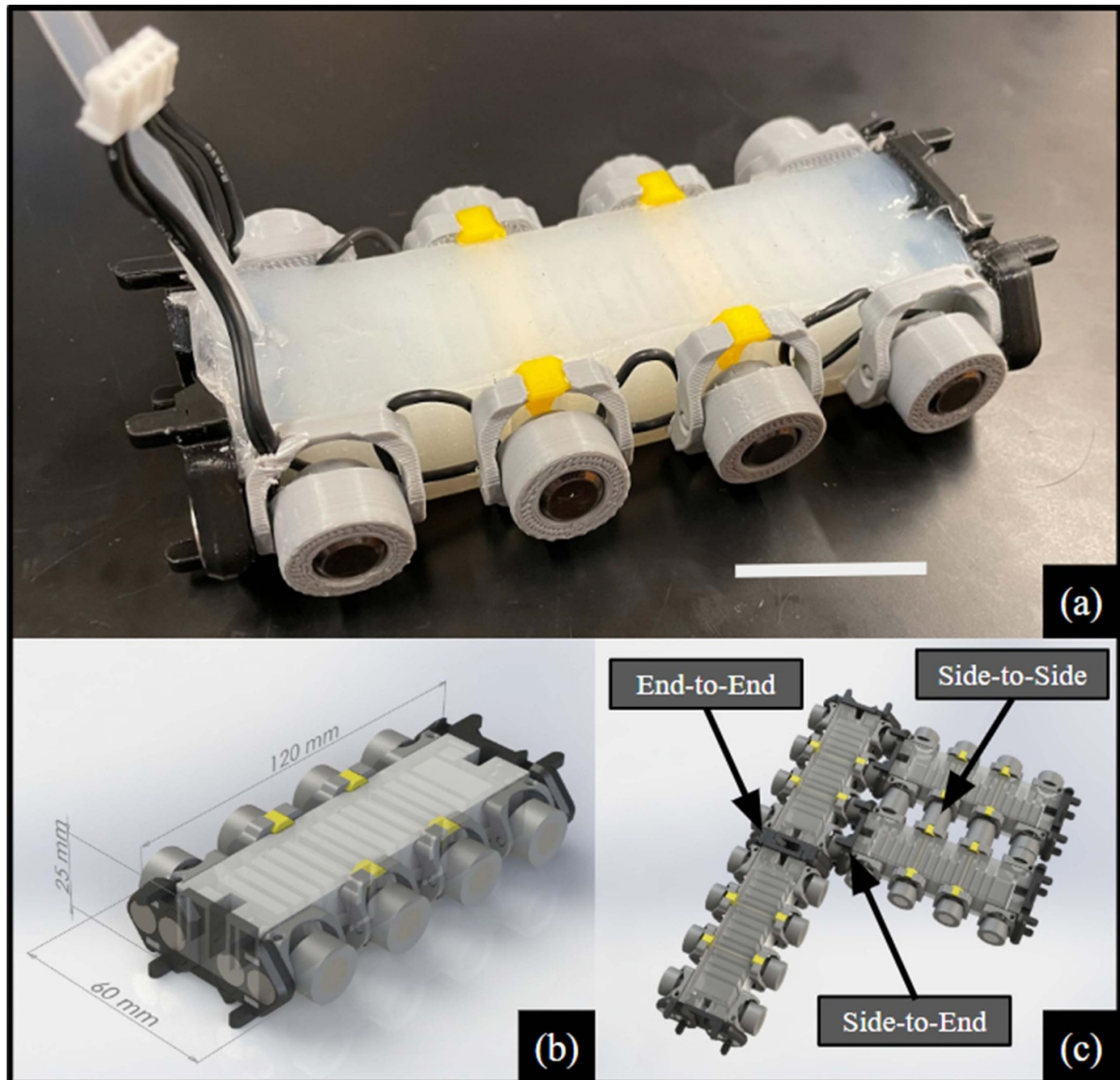


Figure 1. Overview of modular pneumatic actuators and their configurations. (a) Single modular unit used in robot configuration. (b) 3D model of modular unit with dimension units showing the size. (c) 3D model demonstrating four modular units attached to one another utilizing the side and end magnets. The three types of inter-unit connections are indicated. Scale bar: 30 mm.

and the unique soft actuator design that enables tunable interlocking to achieve enhanced grasping abilities. The implemented modular pneumatic actuators (MPAs) use novel designs of side magnets and hinges that allow for end-to-end, side-to-side, and especially side-to-end connections, which have not been previously demonstrated on similar soft robots. Furthermore, the design of the PMCs allows novel tunable interconnectivity between the actuator units. These PMCs open up new possibilities for controlled and autonomous connectivity between the actuators for modular robots. Compared to other soft systems with passive connectivity [37], active disconnection mechanism [8], or limited abilities to connect only at the tips, the presented modular robot can actively disconnect, tune the inter-module connectivity strength, and enable inter-module connections at both their tips and sides. The enhanced connectivity allows both parallel and series

assembly of elemental soft actuators to form planar or complex spatial robotic configurations. The developed connection mechanism increases the number of achievable robotic configurations, enabling a greater variety of tasks that can be accomplished using a single robotic system. In addition, these advanced connecting capabilities allow the robot to modulate its stiffness by configuration alteration or strength modification, making it ideal for grasping various shaped objects or conforming to its surroundings. The developed concept of stiffness modulation and structural reconfiguration can be applied to other modular systems of various scales (e.g. micro and macro) with locomotion and structure forming capabilities [20–22]. The demonstrated soft reconfigurable robots have the potential to be used in automated industrial applications, agriculture, collaborative robotics, manufacturing, medical robotics, space robotics, and search and rescue missions [1–3].

In the remainder of this paper, we first discuss the design, construction, and control of the elemental soft actuators. Next, we show the characterization of the PMCs, which are the crucial elements of the articulating inter-module connectivity and discuss the modularity considerations in the design of these modular actuators. Following, we discuss the experimental results and characterization of the elemental soft actuator units that are used for grasping and constructing the ManusBot configuration. We demonstrate the effective bending capabilities, strength, and operating conditions of these individual modular units. Stiffness for various multi-actuator configurations is calculated and compared to the experimental results to demonstrate robots' stiffness modulation capabilities. Afterwards, we present the robots' grasping capabilities for various predetermined spatial actuator configurations with and without utilizing the inter-unit connectivity. Then, we demonstrate ManusBot's ability to grasp and handle objects of various sizes and weights. Last, we discuss alternative future uses of these modular actuators, their advantages and limitations compared to other modular soft robots and potential impacts on the soft robotics field, and their potential applications.

2. Methods

2.1. Elemental actuator design

All robot configurations discussed in this paper are composed of identical MPAs (figure 2). These actuators, with carefully designed geometry and selected dimensions, are constructed to allow for modularity. As each unit is 120 mm long, 60 mm wide, and 25 mm thick, these units can interconnect with one another end-to-end, side-to-side, or side-to-end (two units per side). The PMCs at the sides have mechanical hinges that can swivel $\pm 60^\circ$, allowing for an articulating connection and easy morphology reconfigurations. Each actuator contains miniature permanent magnets which allow module connection in deformed or undeformed states to form various flexible structures. The locking tabs at the ends (front/rear) allow secure locking to strengthen these connections (figure 2(a)). These tabs also limit the range of motion of the mechanical hinges when connected side-to-end as in the ManusBot configuration discussed in section 3.4, increasing the rigidity and strength of the structure.

The MPAs are actuated using a positive air pressure. The upper section of the actuator consists of a series of air chambers which expand under air pressure (figure 2(b)). The inextensible mesh layer molded in the bottom layer allows deflection of the actuator in one direction (figure 2(b)). The thickness of the side and top walls of the actuator were optimized to minimize side wall expansion and maximize bending actuation despite the embedded hard components.

The PMCs are crucial in the attachment/detachment of actuator units with one another. Each PMC unit consists of a permanent magnet and an electromagnet coil wrapped around a carbon steel core (figure 2(d)). When an electric current is applied through the coil, the created variable magnetic field can cancel out or strengthen the overall resulting magnetic

field, depending on the direction of the current. The benefit of using these PMCs is the reduced power required to connect the modular units, as the permanent magnets are naturally attracted to each other to form connections. Power is only needed for disconnection (when units are previously connected), reconnection (when units are not connected but sufficiently close), or to strengthen the connection (when units are already engaged and increased force capacity is needed).

2.2. Actuator construction

We designed and fabricated the flexible pneumatically driven soft actuator modules (figure 1(a)). The soft actuators use a pneumatic network design and are made of Dragon Skin 10 (Smooth-On, Inc., Macungie, PA) silicone rubber (figure 3). The actuators were fabricated using a two parts mold to create an upper pneumatic chamber portion as well as a lower solid layer with embedded sheet of fiberglass mesh as an inextensible layer and plastic supports for hinge housings (figures 3(b) and (c)). The two parts were fused together using additional silicone rubber (figure 3(d)). All hard components of the units, including the PMC housings, hinges, top and bottom supports, and end connectors were custom designed and 3D printed using polylactic acid material. A $\frac{1}{8}$ inch hose fitting was embedded into one end of the unit and the 3D printed ends with permanent magnets were glued onto the soft actuators using the same silicon material (figure 3(e)). The PMC hinge housings were secured onto the embedded (top and bottom) supports that are placed through the soft actuator (figure 3(f)). These are structural supports that hold the hinges and PMCs in place (figure 3(g)).

The PMCs were constructed using 24-gauge wire, a carbon steel core (6 mm in diameter and 8 mm thick), and a 3D printed housing (figure 2(d)). A 1.8 m wire is wrapped around the carbon steel core in about 80 turns clockwise from the front of the PMC. The wire coil and core are placed into a housing and secured with a 3D printed cover. Two neodymium magnets (10 mm in diameter and 2 mm thick each) are placed on the rear of the PMC, directly onto the carbon steel core. The PMCs are snapped into the hinge housings (figure 3(g)). Four PMCs on each side of the unit are wired in series. To characterize and identify the ideal configuration of the PMC, we varied the PMC designs using different wire gauge and number of magnets. Overall, three different configurations of PMCs were constructed using one or two neodymium permanent magnets with wire thicknesses of either 24 or 30 gauge. The magnetic coil size had to remain the same (15 mm in diameter and 6 mm in thickness) to preserve the form factor of the PMC, thus the 30-gauge wire had more windings (180 turns) than the 24-gauge (80 turns).

2.3. Actuator control

The benefit of modularity in this design is that each actuator unit can be controlled individually. There are two main components to be controlled: pneumatic actuation and powering of PMCs. Both components are controlled using a single

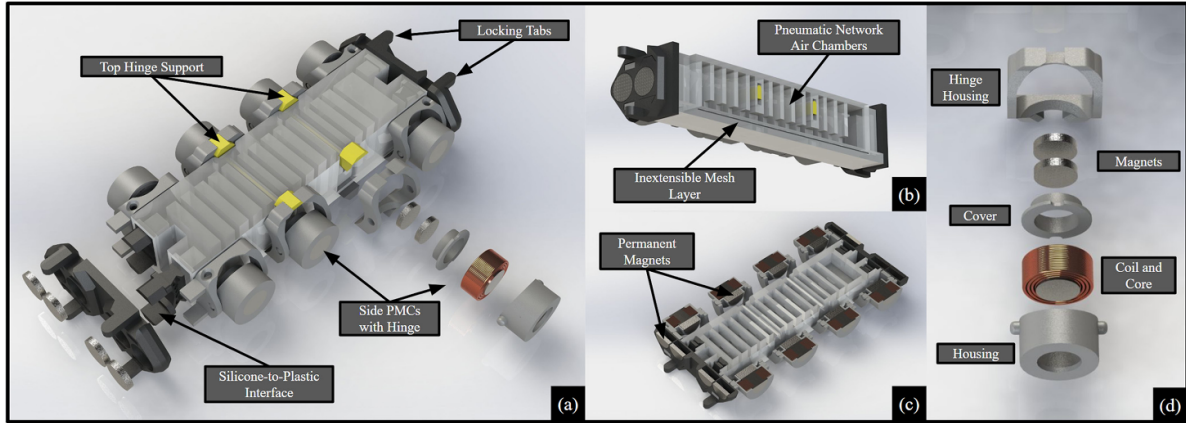


Figure 2. Individual modular pneumatic actuator (MPA). (a) Exploded view of the MPA with indicated side PMCs and hinge supports. (b) Cross-sectional view of modular unit showing the internal air chamber structure of the unit and the embedded inextensible layer. (c) Top cross-sectional view of the MPA showing the internals of the assembled PMCs and air chambers. (d) Breakdown of components used to manufacture PMC, including 3D printed housing, copper winding coil, carbon steel core, two neodymium permanent magnets, and a 3D printed back cover.

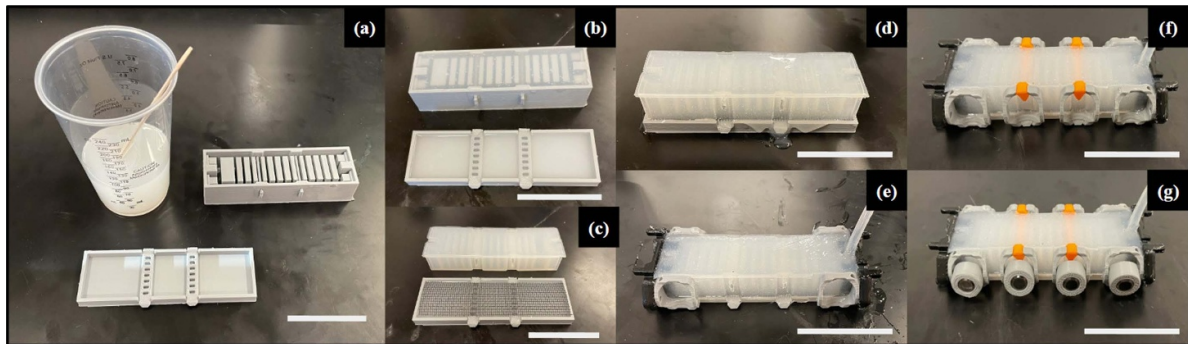


Figure 3. Molding process of soft actuator. (a) 3D printed top and bottom molds ready to be poured with silicone rubber. (b) Molds filled with silicone rubber. (c) An inextensible mesh layer is added to the bottom mold and the top section of the actuator has been removed from the mold. (d) Top section is placed on top of the mesh layer in bottom mold, and the two sections are molded together with silicone rubber. (e) Silicone tubing and unit ends are attached using additional silicone. (f) Top supports are inserted into holes that go through the units and hinges are secured to supports. (g) Final completed MPAs with PMCs added to hinges. Scale bar: 50 mm.

Arduino microcontroller with a Bluetooth module that allows full control of each actuator via a mobile device. For pneumatic control, each unit is connected to a solenoid valve that can be powered on and off with a relay to control the deflection of the actuator. The PMCs on each side of the modular units are connected in series and each side can be powered separately. The use of an H-bridge circuit for each side of the actuator allows for full current control of the PMCs, either to provide power to disengage them or to reverse the current to strengthen the magnetic field and increase the attractive forces between the connected PMCs.

2.4. Magnetic field strength calculation

The use of PMCs allows for decreased power consumption, but the strength of the magnetic field produced by the coils needs to be strong enough to cancel out the magnetic field of the permanent neodymium magnet. To calculate the magnetic field required to cancel the

effect of the permanent magnets, we used the Ampere's Law equation [39]

$$B = \frac{\mu_0 NI}{L}, \quad (1)$$

where B is the magnetic field strength (Tesla), μ_0 is the magnetic permeability of carbon steel taken as $1.4 \cdot 10^{-8}$ ($\text{N} \cdot \text{A}^{-2}$), the ratio N/L is the number of turns per length of the core/shaft (turns per meter), and I is the current flowing through the wire (A).

The measured magnetic field strength of the PMCs with only the permanent magnet and carbon steel core was 34.85 mT. Using the Ampere's Law and the recorded magnetic field strength, it was found that a current of 4.83 A would be needed to cancel out this produced magnetic field. As discussed in more details in Results section, in our experiments, the PMCs' magnetic field was reduced to -0.94 mT with an applied current of 5 A, which indicates that the theoretical calculations and the experimental data match closely.

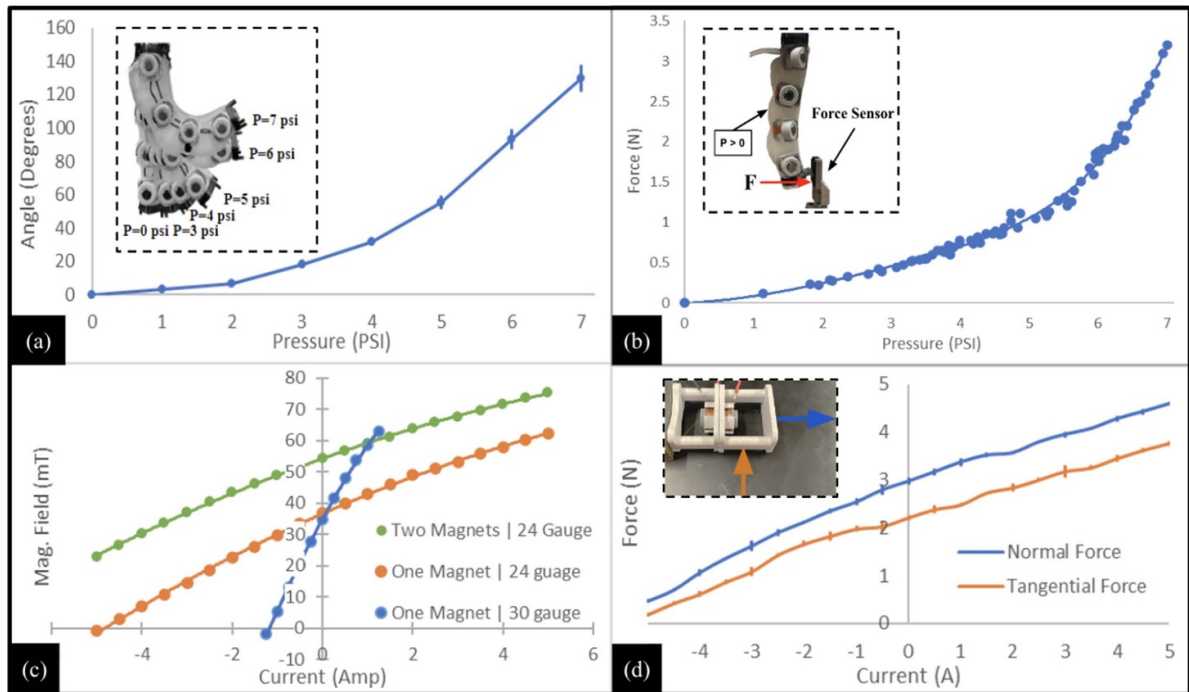


Figure 4. Elemental unit and permanent magnet with coil data. (a) Representative graph of applied pressure and its corresponding angle of deflection. (b) Correlation between pressure and blocking force of a representative actuator showing nonlinear force-pressure relationship based on two repeated tests. The embedded image shows the experimental configuration. (c) The resulting magnetic field testing of PMC with varying applied currents and constructions, including different wire gauge of the coils and the number of permanent magnets. Three tests with different magnets were performed for each variation, standard deviation between tests was too small to represent visually on graph. (d) Tangential and normal forces of PMC at various applied electric currents. Forces were applied to the housing of the units by a force sensor at locations and directions indicated with arrows.

3. Results

3.1. Elemental unit and permanent magnets with coils characterization

We began testing by determining the capabilities of the independent elemental actuators. The pressure-deflection relationship of individual actuators was obtained using a unit that was suspended vertically by end magnets. Figure 4(a) shows the relationship between the applied pressure and the resulting actuator's deflection, with a maximum deflection angle of 120° at an applied pressure of 7 psi (~ 50 kPa). Using pressures greater than 8 psi led to the permanent deformation and failure of the unit; therefore, the maximum operating pressure in all tests was 7 psi. The blocking force was measured in the same configuration with a force sensor (Force Sensing Resistor (0–2.2 lbs.), Honeywell, Charlotte, NC) located at the tip of the actuator blocking the deflection. At a peak pressure of 7 psi, the resulting blocking force was 3.2 N (figure 4(b)).

Three PMC designs were characterized to identify required power to cancel out the magnetic field produced by the permanent magnet. Figure 4(d) shows the measured magnetic field strength at the tip of the PMCs, as measured by a magnetic field meter. The strength of the magnetic field of permanent magnets increased from 35 to 55 mT when increasing the number of magnets in the PMC from one to two. The use of a second permanent magnet allows the PMC to support greater

loads; however, this configuration requires additional current to completely cancel out the magnetic field.

The results in figure 4(c) show that the magnetic field produced by a single permanent magnet within PMC can effectively be canceled out with a current of approximately -5 A or doubled with a current of 5 A. The relationship between the electric current and the magnetic field strength of the PMC was observed to be only slightly nonlinear. The coil constructed with a thinner 30-gauge wire produced a greater magnetic field at a lower current but also generated more heat due to the increased resistance of the thinner wire. Since the PMCs are housed in a plastic casing, the increased heat can induce additional thermal stress to the system, and over longer periods of time, result in structural damages. By comparison, the PMC configuration with 24-gauge wire had lower resistance and produced less heat. In addition, the larger diameter 24-gauge wire also allowed the coils to be powered with a maximum voltage of 8.4 V, which is significantly lower than the 23.2 V needed to power 30-gauge coils. The lower voltage requirement and the reduced heat generation made the 24-gauge wire a preferred option that was later used in our design and all experiments. Though the coil was not able to completely cancel out the PMC that utilizes two magnets, it significantly reduces the force enough to allow for easy disconnection, as seen in the following experimentation.

To determine the effects of the electric current on the normal and tangential (shear) forces between two PMCs, we

employed the experimental setup illustrated in figure 4(d). A fixture with an embedded force sensor was used to pull the two PMCs apart in the normal and tangential directions relative to the face of the magnets. The normal force to separate the PMCs without any applied current was 2.97 N and it nearly doubled to 4.6 N when 5 A of current was applied. When a current of -5 A was applied, the normal force was reduced to around 0.6 N, which would allow for easy separation of the PMCs from one another. While the tangential forces of the magnets also increased with current, the rate of increase was slower, and the maximum value of 3.76 N was reached at an applied current of 5 A. Furthermore, the normal force exceeded the tangential force at all current levels. This observation indicates that the strengths of modular configurations are direction dependent, meaning that a multi-actuator robot configuration that leverages interconnection forces in a normal direction will be stronger than a similar system that relies on shear forces.

3.2. Configuration and stiffness modulation

The versatility of the MPAs allows them to form many structures with varying stiffnesses for a wide range of applications. To demonstrate this, we arranged these units in five set configurations to test their resulting stiffness using a force-displacement method, showing the range of controllable mechanical properties such as flexibility and rigidity (figure 5). With the single unit serving as a control (figure 5(b)), the other four set configurations (figures 5(c)–(f)) consisted of multiple (2–4) units aligned with one another and connected via their side magnets. The concentrated load was applied to these structures as shown in figures 5(b)–(f). The linear configurations with actuators connected in parallel (figure 5(c)) showed a much lower stiffness and higher compliance when compared to the angled and closed-form structures (figures 5(d)–(f)), as demonstrated by the initial slopes of the force-displacement curves in figure 5(a). By connecting the units at a 90° angle using the hinges, the stiffness of the formed structure increased significantly when compared to that of the linearly connected structures (0° angle). Specifically, the two-unit angled configuration (figure 5(d)) showed a high degree of bending stiffness ($k_b = 110 \text{ N m}^{-1}$) during the initial bending displacement of approximately 10 mm as compared to the stiffness $k_b = 42 \text{ N m}^{-1}$ of the linear two-unit configuration (figure 5(c)). These experimentally measured bending stiffnesses for both angled and linear configurations closely matched the theoretically calculated values of 118 and 44 N m^{-1} , respectively (see section 3.3 and figure 5(g)). However, as the load increased and the angled structure became more displaced, the configuration changed from angular to nearly linear, due to the flexibility in hinges, which resulted in reduced stiffness at larger displacements.

In addition, we evaluated the performance of the two closed-form structures (i.e. square and diamond) (figures 5(e) and (f)). The closed-form square structure (figure 5(e)) has the highest moment of inertia (MOI) and theoretical bending stiffness (see section 3.3), which suggested the highest structural rigidity. However, this configuration relied mostly on the tangential (shear) strength of the magnets rather than the rigidity

of the structure. Therefore, as the applied load and displacement increased, the magnets became disengaged, resulting in reduced stiffness and lower force capabilities. The closed-form structures which demonstrated higher stiffness are intended for applications where no movement of actuators is necessary. These structures can be applied to situations where the robot is required to lift or move bulky objects that cannot be grasped by traditional means. The stiffening of the structure allows a normally soft robot to become more rigid, opening up more possibilities for its application in the workspace.

An increase in structural stiffness was achieved by rotating the closed-form square structure by 45° to form a diamond structure (figure 5(f)). This rotated configuration relied more on the normal forces of the PMCs as opposed to the tangential forces as the concentrated load was applied in line with the magnets. As a result, the experimentally obtained stiffness increased from 219 N m^{-1} for square to 300 N m^{-1} for diamond configurations. We further investigated the effect of the applied electric current in the PMCs to investigate the maximum structural stiffness of the diamond configuration. A current of 3 A was applied to further strengthen the connections between the PMCs, resulting in an increased force (6.5 N at 30 mm displacement) required to separate the magnets and units. This configuration had the same initial stiffness as the unpowered diamond configuration; however, the engagement of the magnets allowed the structure to maintain its shape under higher forces. The stiffness modulation achieved through unit structural reconfiguration clearly demonstrates the advanced capabilities of the soft robotic actuators.

3.3. Stiffness value calculation

We determined the effective elastic modulus, E , of the MPAs from the bending stiffness test (figure 5) with E defined as:

$$E = \frac{1}{3} \frac{FL}{xI}, \quad (2)$$

where F is the measured pushing force, L is the length (120 mm) of the actuator where force was applied, x is the displacement, and I is the MOI [39].

The MOI for each of the different configurations was estimated based on the cross section of the specific configuration and the arrangement of the units (figure 6(a)). The linear portion of the force-displacement relationship shown in figure 5(a), taken as displacement range from 0 to 10 mm, was used to calculate each of the configurations' stiffness obtained from experiments. The force applied to the configuration at a displacement of 10 mm was used in the calculation. The average elastic modulus of elemental MPAs was calculated to be 17.7 kPa. Using this value and equation (2), the stiffness value can be calculated for any number of configurations of ManusBot without the need to test it experimentally.

Figure 6 summarizes the calculated MOI values used for finding the theoretical stiffness of each configuration. The MOI, generally used as a simple measure of a structure's cross-sectional capacity to resist bending motion, is dependent on the shape of the structure. In our analysis, the MOI affects how much of a force/moment will be needed to

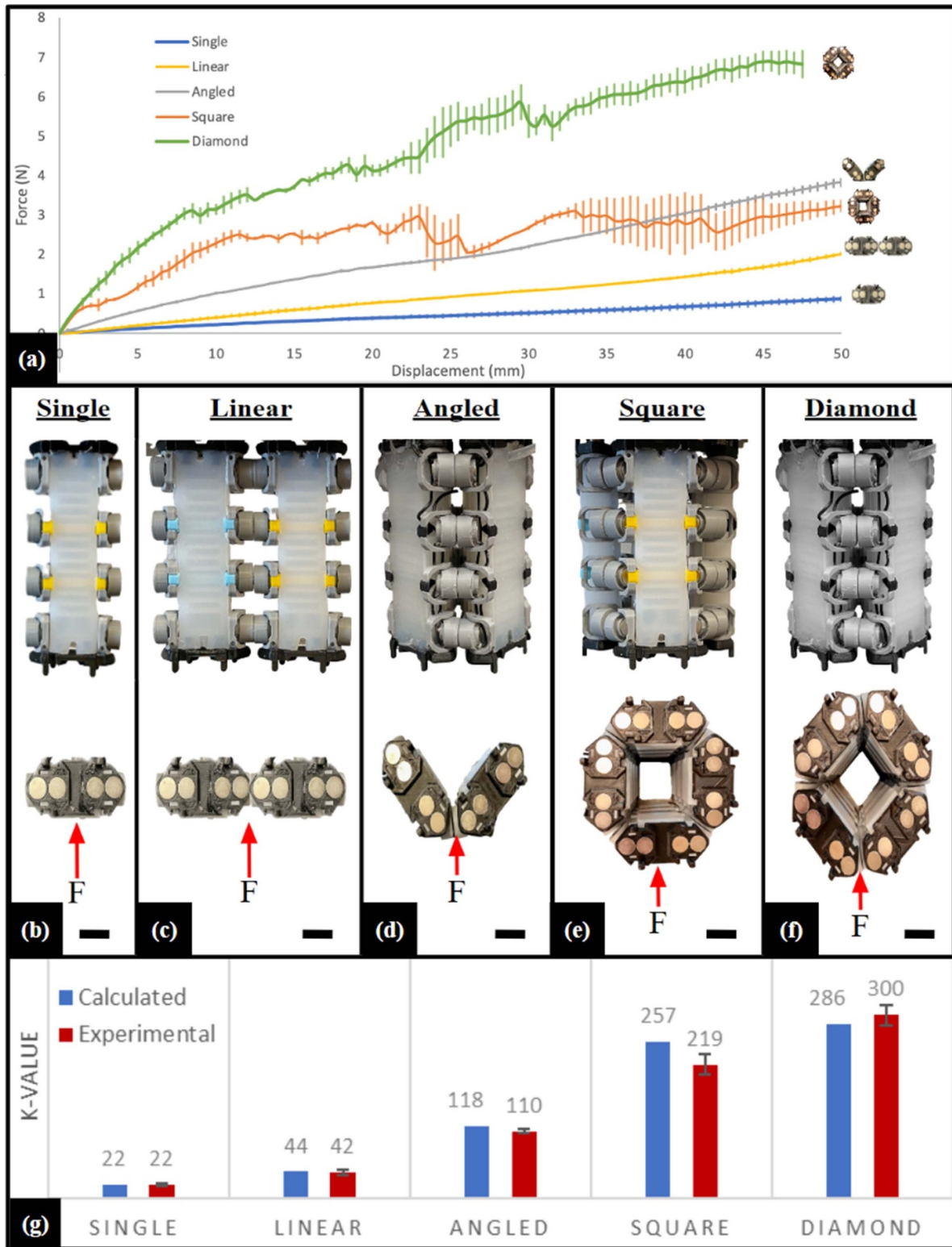


Figure 5. Stiffness configurations used for analysis. (a) Stiffness data collected from five tested configurations showing their force-displacement curves. The configurations tested include (b) a single unit, (c) two units connected linearly (0° angle), (d) two units angled at 90° , (e) four units in a square configuration, and (f) four units rotated to form a diamond shape configuration. All configurations show applied location of force F. (g) Comparing the experimental and calculated stiffness values of the five tested configurations. Scale bar: 25 mm.

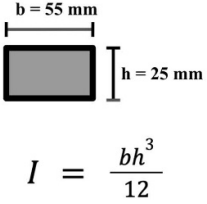
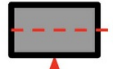
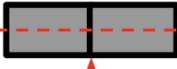
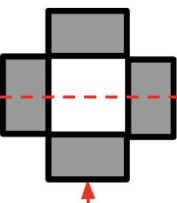
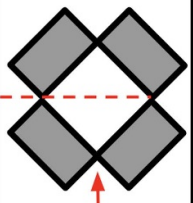
Configuration	Single	Linear	Angled	Square	Diamond
 $I = \frac{bh^3}{12}$					
Moment of Inertia (m⁴)	I = 7.16E-08	I = 1.43E-07	I = 4.29E-07	I = 8.36E-07	I = 8.31E-07
Force at 10mm (N)	F = 0.22	F = 0.42	F = 1.1	F = 2.19	F = 3.1
k-Value	22	44	118	257	286

Figure 6. Stiffness calculation for various MPA configurations. Table showing the configurations used for calculating their effective stiffness values k . Moment of inertia was calculated based on the number and orientation of units, as illustrated with simplified schematics. The force values were taken from configuration testing at 10 mm of displacement.

bend a structural configuration. The MOI was calculated by simplifying the unit to a homogeneous solid geometric shape. The simplest configuration was a single actuation unit. Its MOI was calculated using the following equation $I = \frac{bh^3}{12}$, where b and h are the width and height of the unit, respectively. For other configurations, appropriate MOI equations were used to accommodate the different orientations and the number of units in the structure. Next, the calculated MOI and the applied force were used in equation (2) to determine the Young's modulus of a single actuator unit. It is worth noting that the number alone does not represent the characteristics of any specific material, but rather it represents the effective properties of a singular unit. Using the calculated Young's modulus, the stiffness value k was calculated for each configuration. This calculated value was compared to the experimental stiffness data collected for all configurations.

Using the Young's modulus calculated, the stiffness of other configurations, even if they have not been fabricated and tested, can be estimated. An example is a repeating angle (corrugated) structure, which has not been tested experimentally; however, its effective stiffness value can be obtained using the analytical method described above. This approach can help engineers design structures or module configurations for applications with specific stiffness requirements without the need for trial and error.

3.4. Grasping capabilities and strength

The modular units can be configured in multiple ways for various grasping capabilities. Multiple experiments were performed using these configurations for grasping objects. These configurations can be divided into three main groups: pinching (2 units), disconnected square (4 units), and connected

square (4 units), as shown in figures 7(a)–(c). With a pinching formation, the two units were able to grasp a variety of objects of different weights, shapes, and sizes (figures 7(d) and (e)). We evaluated the maximum load bearing capacity (i.e. the maximum weight of the objects) during grasping tasks for the two-unit and four-unit configurations (see figure 7(h)). The two-unit configuration (figure 7(a)) was able to support forces of up to 3.1 N before the object slipped. In a square configuration with all four units completely disconnected (figure 7(b)), the robot was able to support a weight/force of 3.9 N. When the PMCs on all sides were fully connected (figure 7(c)), the load capacity of the robot increased to 5.8 N, which is nearly twice of that in the pinching configuration. It is important to note that in these configurations, the size of objects that can be grasped are limited to the aperture of the robot. The engagement of the PMCs was shown to keep the actuators closer to the grasped object under pressure, allowing them to hold the object with a higher force. The results obtained in figure 7(h) are based on objects of similar shapes and sizes. The higher weight capacity of the connected square configuration highlights the advantages of using the side PMCs.

ManusBot is a modular soft robot constructed of two to four elemental soft actuator units arranged (connected or disconnected) in parallel, all of which are attached to the sides of two additional units to form a hand-like configuration (figure 8(a)). The independent control of the top actuators can shape and tailor the gripper configuration that enables grasping of objects with a broad range of shapes and sizes. ManusBot can wrap around long objects and grasp a tall, soft inflated bag (figures 8(b) and (c)) or pick up a small rigid object (figure 8(d)). The measured holding force in this configuration was measured to be 1.16 ± 0.22 N. Because ManusBot can wrap around the objects it is grasping, this configuration

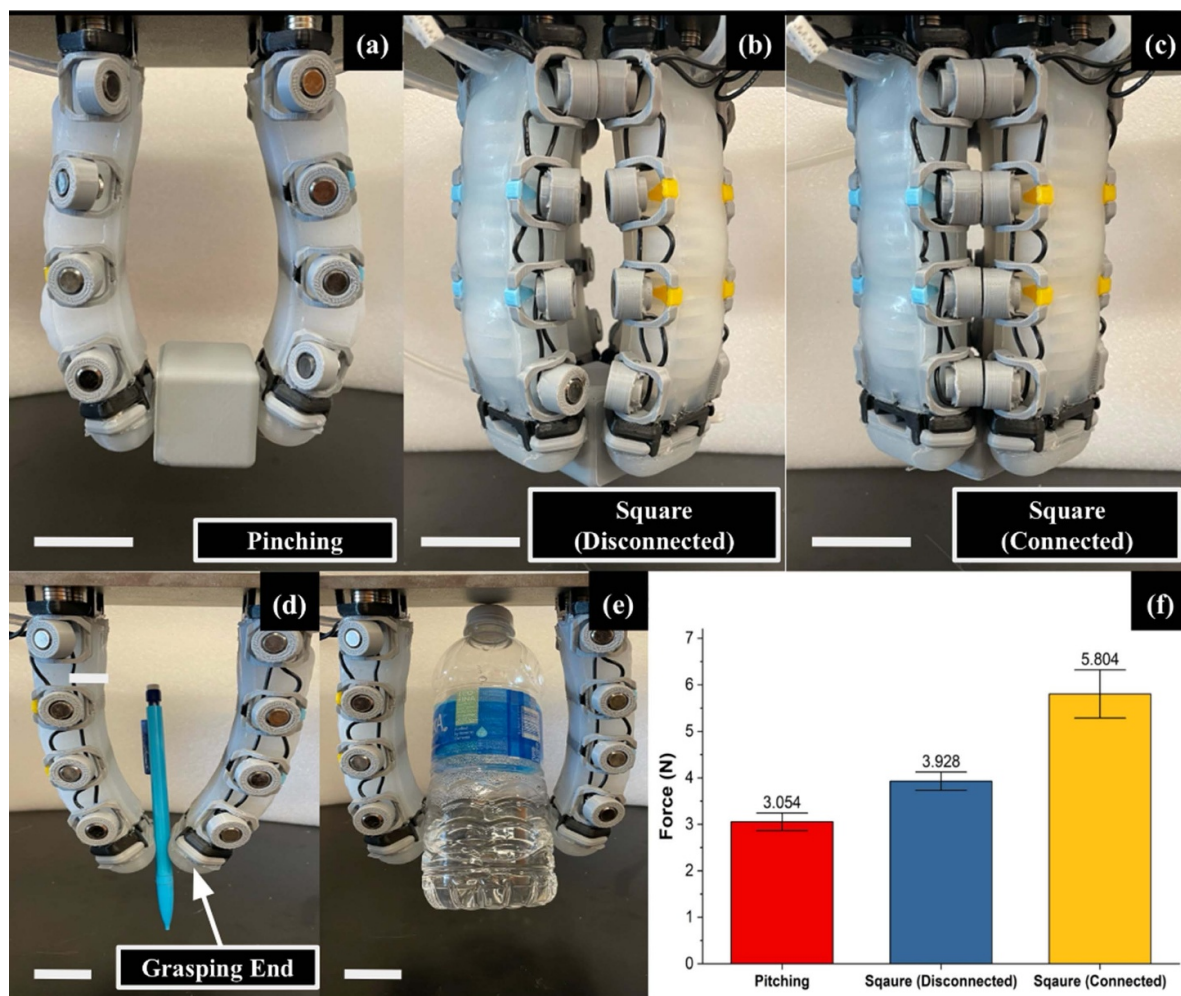


Figure 7. Grasping configuration testing. (a) Pinching configuration while grasping a 3D printed cube. Square configuration grasping a 3D printed cube with (b) disconnected and (c) connected side PMCs. The weight of the 3D printed cube is 15 grams and was accounted for in grasping force. ManusBot grasping (d) a pencil and (e) a water bottle. (f) ManusBot grasping force for two-unit pinching and four-unit square configurations in both disconnected and connected states. Scale bar: 30 mm.

is able to pick up tall objects (taller than the robot itself) without interfering with actuation. Figure 8(d) demonstrates ManusBot's abilities and the order-of-operation with a time sequence of picking up a 3D printed object.

The true uniqueness of the ManusBot lies in its ability to adapt its shape and strength on demand, depending on the weight, shape, and size of the objects being handled. Figures 8(e)–(g) demonstrate the novelty of ManusBot's reconfiguration abilities by grasping an object of larger size and weight that cannot be grasped in its initial configuration. When the actuators are configured to form a closed-form (square/diamond) structures with engaged PMCs and applied pneumatic pressure, the structural stiffness significantly increases. Such robot configurations can be used for load-bearing applications where minimal deformation of units is expected. By altering its structural configuration and stiffness properties, the ManusBot can hold objects with unique shapes (e.g. through body insertion in an opening in the demonstrated example). Our findings demonstrate ManusBot's increased grasping potential, thus underscoring

its remarkable versatility and expanded functionality. By tailoring its form and strength to various tasks, the ManusBot offers a promising new approach to robotic manipulation in a range of settings.

4. Discussion

Here we discuss the implications of the modular actuator concept in terms of its capabilities and possible applications as a versatile grasping soft robot. There are numerous uses of these MPAs outside of the demonstrated configurations. The modular design allows these actuators to easily connect to one another in ways that are best tailored for specific applications. Modularity increases the usefulness of the soft robot system and can help eliminate the need for users to buy multiple task specific devices or robots. The versatility of the modular soft robot can be further expanded by increasing the load capacities through other interunit connection methods, such as an end-to-end connection to create a snake-like robot using the same modular actuators.

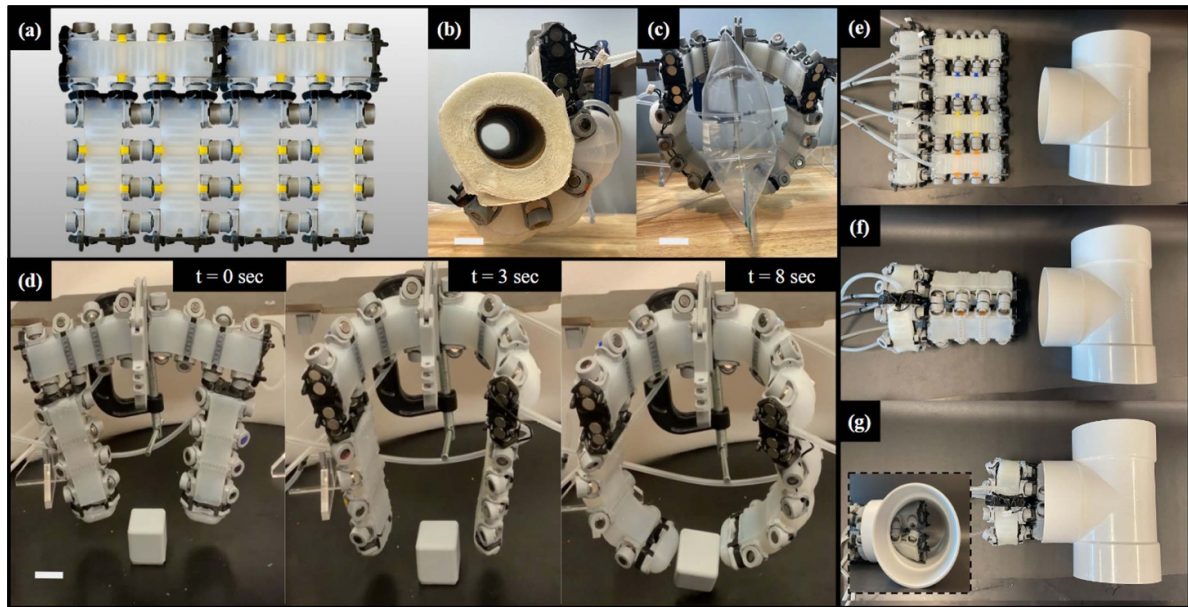


Figure 8. ManusBot grasping various objects. (a) ManusBot soft robot constructed from six modular soft units. ManusBot grasping (b) a paper towel roll and (c) a tall, inflated plastic bag. (d) Time sequence of ManusBot bending and picking up a 3D printed cube in the pinching configuration. (e) ManusBot before reconfiguration and a 4-inch PVC fitting. (f) ManusBot reconfigured into a square configuration. (g) ManusBot inserted into PVC fitting and inflated to grasp fitting. The embedded image shows ManusBot digits inflated inside PVC. Scale bar: 30 mm.

The use of magnets on both ends of the elemental MPAs allows for quick changes of the actuator units or adding/removing custom grasping end units, as seen in figure 7. Due to the modular capability of these actuators, it is possible to use custom-designed grasping ends that can be quickly fabricated and attached to the robot to allow grasping of uniquely shaped objects in specific applications. For example, for very small parts, smaller rubberized grips can be attached to allow for more precise grasping. It may even be possible to attach additional PMCs to a custom attachment to allow for the grasping of metallic objects, from large and heavy (e.g. beams) structures to small and light parts (e.g. screws) in an assembly line.

The proposed soft reconfigurable robots have the potential to be used in a wide variety of applications, including automated industrial operations, collaborative robotics, manufacturing, medical robotics, space robotics, and search and rescue missions [9]. ManusBot can be used in automation environments, performing a variety of repetitive tasks such as sorting and moving objects of various shapes and sizes. The modularity of this design allows for the purchase of a single robot to complete multiple task-specific operations on an assembly line, saving money for the end users by eliminating the need to buy different machines for these tasks [40]. The soft nature of the design allows the robot to grasp and move fragile and delicate objects such as fresh produce or glassware. Lastly, this design has great potential in education and training purposes by introducing students to numerous soft robotics principles such as pneumatic actuation, magnetic devices, control methods, and object manipulation [41]. Its modular design makes it a great learning tool in a similar way to how LEGO inspires creativity in children. Students can be highly creative,

yet provided with additional design freedom, to engineer their own robots using these modular units.

In this growing field of modular soft robots, many other designs have emerged, each showcasing distinct advantages and limitations. While some modular soft robots focus on achieving specific functionalities or morphologies, others prioritize adaptability and reconfigurability. Our modular robot design stands out from these alternatives through its unique side and end magnetic connections, allowing for actuator-to-actuator connections instead of an attachment to a specially designed rigid base. This feature enables our modules to exhibit a high degree of reconfigurability and adaptability for versatile tasks. Another notable feature is the unique capability to modulate stiffness through reconfiguration, an ability not observed in other modular soft robots. Furthermore, our actuator typically operates at lower pressures and yields higher force output compared to alternative designs (see table 1). Nevertheless, it is important to acknowledge the inherent trade-offs associated with our design, such as the increased weight due to the additional magnets and rigid components. Additionally, the softer and more compliant nature of our modules, while allowing for lower operational pressures, can lead to gravitational sagging when configured in complex formations, posing challenges in maintaining desired configurations over extended periods. Despite these drawbacks, the innovative features of our modular soft actuators allow for enhanced versatility and performance in diverse applications, highlighting the ongoing evolution and exploration within the field.

The current system also has several limitations. The usefulness of these soft actuators varies greatly with the scale at which they are produced [16]. The scaling of these units is

Table 1. Comparison of existing modular soft robotic actuators.

	Notable capabilities	Connectivity	Blocked force	Bending angle	Operating pressure	References
Modular pneumatic actuator, ManusBot	High configurability, variable stiffness, shape adaptability	Actuator-to-actuator, base-to-actuator	3.2 N	130°	55 kPa	This work
SoBL, Fast-build modularized design block	Mechanical connection, high configurability	Actuator-to-actuator, base-to-actuator	1.22 N	110°–250°	25–55 kPa	[13]
3D printed modular soft gripper with metamaterial	Shape conformity	Base-to-actuator	1.94 N	120°	150 kPa	[14]
Soft hands with magnetic elements	Variable stiffness	Base-to-actuator	N/A	N/A	10 kPa	[21]
3D printed soft gripper	N/A	Base-to-actuator	N/A	104°	50 kPa	[15]
Soft modular robot with docking	High configurability, three degrees-of-freedom	Actuator-to-actuator	N/A	180°	110 kPa	[12]

limited by the strength of the permanent magnets and the size of the electromagnets needed to cancel out the magnetic field. As the units get larger, the mass of each unit will increase, and a stiffer pneumatic actuator would be needed. This can be overcome either by altering the material they are made of (e.g. using elastomers with higher hardness) or by altering the structure they are molded from. The design also consists of multiple hard components that could limit applications where these robots can be used as these add weight and rigidity to the units that can affect their safety and functionality. We acknowledge that our design has not yet been optimized for weight and material/component selection, which is a limitation of our current design. However, when compared to the performance of other soft fluidic actuators [9], our actuator was able to double the generated force (3 N) at 1.5 times lower pressure (7 psi), which results in increased safety of operation due to lower pressures. Lastly, the current actuator design is tethered with pressurizing tubes and electric wires. However, continued miniaturization of components, use of flexible electronics and micropumps, integration of soft and flexible materials, and on-board power supplies can potentially enable untethered, standalone designs. Integration of soft and flexible materials to replace rigid components can enable creation of completely soft modular robots. Future iterations of this design may show smaller, lighter, untethered, softer, and more versatile robotic actuators which can be used in precision-based applications.

In summary, our soft robotic actuator's modular design allows the robot system to be used in a great number of ways. One of the main advantages of our design is its novel interlocking mechanism that allows the units to be interconnected. We have demonstrated a configuration, ManusBot, that can be formed using multiple modules utilizing their magnets and PMCs. We have demonstrated ManusBot's abilities to

modulate its stiffness by altering the structural configuration and to grasp objects of various shapes, sizes, and materials. The modular soft pneumatic actuators used to construct the ManusBot can be reconfigured into many other robotic designs for versatile applications, from search and rescue to manufacturing, due to their high modularity and the vast possibilities in structural configurations.

Data availability statement

The data that support the findings of this study are available upon reasonable request from the authors.

Acknowledgments

This material is based upon work supported by the National Science Foundation under Grant No. 2235647.

Conflict of interest

The authors declare no conflict of interests.

Author contributions

M T: conceptualized and designed the study and directed the project. J K: designed and built the robot, performed the testing, and wrote the original draft of the manuscript. M T and W X: provided directions and revised and edited the manuscript. J K, W X, and M T: analyzed the data and interpreted and discussed the results.

ORCID iDs

Joshua Knospler  <https://orcid.org/0009-0005-4614-6616>

Wei Xue  <https://orcid.org/0000-0001-6550-5366>

Mitja Trkov  <https://orcid.org/0000-0001-8556-7214>

References

- [1] Zhang B, Xie Y, Zhou J, Wang K and Zhang Z 2020 State-of-the-art robotic grippers, grasping and control strategies, as well as their applications in agricultural robots: a review *Comput. Electron. Agric.* **177** 105694
- [2] Kim U, Jung D, Jeong H, Park J, Jung H-M, Cheong J, Choi H, Do H and Park C 2021 Integrated linkage-driven dexterous anthropomorphic robotic hand *Nat. Commun.* **12** 1–13
- [3] Truby R L, Katzschmann R K, Lewis J A and Rus D 2019 Soft robotic fingers with embedded ionogel sensors and discrete actuation modes for somatosensitive manipulation *2019 2nd IEEE Int. Conf. on Soft Robotics (RoboSoft)* pp 322–9
- [4] Rus D and Tolley M T 2015 Design, fabrication and control of soft robots *Nature* **521** 467–75
- [5] Mosadegh B, Polygerinos P, Keplinger C, Wennstedt S, Shepherd R F, Gupta U, Shim J, Bertoldi K, Walsh C J and Whitesides G M 2014 Soft robotics: pneumatic networks for soft robotics that actuate rapidly (*Adv. Funct. Mater.* 15/2014) *Adv. Funct. Mater.* **24** 2109
- [6] Polygerinos P, Correll N, Morin S A, Mosadegh B, Onal C D, Petersen K, Cianchetti M, Tolley M T and Shepherd R F 2017 Soft robotics: review of fluid-driven intrinsically soft devices; manufacturing, sensing, control, and applications in human-robot interaction *Adv. Eng. Mater.* **19** 1700016
- [7] Manti M, Cacucciolo V and Cianchetti M 2016 Stiffening in soft robotics: a review of the state of the art *IEEE Robot. Autom. Mag.* **23** 93–106
- [8] Kwok S W, Morin S A, Mosadegh B, So J-H, Shepherd R F, Martinez R V, Smith B, Simeone F C, Stokes A A and Whitesides G M 2014 Magnetic assembly of soft robots with hard components *Adv. Funct. Mater.* **24** 2180–7
- [9] Zhang C, Zhu P, Lin Y, Jiao Z and Zou J 2020 Modular soft robotics: modular units, connection mechanisms, and applications *Adv. Intell. Syst.* **2** 1900166
- [10] Robla-Gómez S, Becerra V M, Llata J R, González-Sarabia E, Torre-Ferrero C and Pérez-Oria J 2017 Working together: a review on safe human-robot collaboration in industrial environments *IEEE Access* **5** 26754–73
- [11] McKenzie R M, Barraclough T W and Stokes A A 2017 Integrating soft robotics with the robot operating system: a hybrid pick and place arm *Front. Robot. AI* **4** 39
- [12] Zhang Y, Zheng T, Fan J, Li G, Zhu Y and Zhao J 2019 Nonlinear modeling and docking tests of a soft modular robot *IEEE Access* **7** 11328–37
- [13] Lee J-Y, Kim W-B, Choi W-Y and Cho K-J 2016 Soft robotic blocks: introducing SoBL, a fast-build modularized design block *IEEE Robot. Autom. Mag.* **23** 30–41
- [14] Tawk C, Mutlu R and Alici G 2022 A 3D printed modular soft gripper integrated with metamaterials for conformal grasping *Front. Robot. AI* **8** 799230
- [15] Wang Z, Chaturanga D S and Hirai S 2016 3D printed soft gripper for automatic lunch box packing *2016 IEEE Int. Conf. on Robotics and Biomimetics (ROBIO)* pp 503–8
- [16] Li S, Awale S A, Bacher K E, Buchner T J, Della Santina C, Wood R J and Rus D 2022 Scaling up soft robotics: a meter-scale, modular, and reconfigurable soft robotic system *Soft Robot.* **9** 324–36
- [17] Onal C D and Rus D 2012 A modular approach to soft robots *2012 4th IEEE RAS & EMBS Int. Conf. on Biomedical Robotics and Biomechanics (BioRob)* pp 1038–45
- [18] Kurumaya S, Phillips B T, Becker K P, Rosen M H, Gruber D F, Galloway K C, Suzumori K and Wood R J 2018 A modular soft robotic wrist for underwater manipulation *Soft Robot.* **5** 399–409
- [19] Liang G, Luo H, Li M, Qian H and Lam T L 2021 FreeBOT: a freeform modular self-reconfigurable robot with arbitrary connection point—design and implementation *2020 IEEE/RSJ Int. Conf. on Intelligent Robots and Systems (IROS)* pp 6506–13
- [20] Robertson M A and Paik J 2017 New soft robots really suck: vacuum-powered systems empower diverse capabilities *Sci. Robot.* **2** eaan6357
- [21] Marullo S, Salvietti G and Prattichizzo D 2022 On the use of magnets to robustify the motion control of soft hands *IEEE Robot. Autom. Lett.* **7** 11743–50
- [22] Usevitch N S, Hammond Z M, Schwager M, Okamura A M, Hawkes E W and Follmer S 2020 An untethered isoperimetric soft robot *Sci. Robot.* **5** eaaz0492
- [23] Dong Y, Wang L, Xia N, Yang Z, Zhang C, Pan C, Jin D, Zhang J, Majidi C and Zhang L 2022 Untethered small-scale magnetic soft robot with programmable magnetization and integrated multifunctional modules *Sci. Adv.* **8** eabn8932
- [24] Luo M, Wan Z, Sun Y, Skorina E H, Tao W, Chen F, Gopalka L, Yang H and Onal C D 2020 Motion planning and iterative learning control of a modular soft robotic snake *Front. Robot. AI* **7** 599242
- [25] Sui X, Cai H, Bie D, Zhang Y, Zhao J and Zhu Y 2020 Automatic generation of locomotion patterns for soft modular reconfigurable robots *Appl. Sci.* **10** 294
- [26] Shah D S, Powers J P, Tilton L G, Kriegman S, Bongard J and Kramer-Bottiglio R 2021 A soft robot that adapts to environments through shape change *Nat. Mach. Intell.* **3** 51–59
- [27] Althoefer K 2018 Antagonistic actuation and stiffness control in soft inflatable robots *Nat. Rev. Mater.* **3** 76–77
- [28] Must I, Sinibaldi E and Mazzolai B 2019 A variable-stiffness tendril-like soft robot based on reversible osmotic actuation *Nat. Commun.* **10** 344
- [29] Yang Y, Li Y and Chen Y 2018 Principles and methods for stiffness modulation in soft robot design and development *Bio-Des. Manuf.* **1** 14–25
- [30] Gilpin K, Knaian A and Rus D 2010 Robot pebbles: one centimeter modules for programmable matter through self-disassembly *2010 IEEE Int. Conf. on Robotics and Automation* pp 2485–92
- [31] Zhang Z, Heron J T and Pena-Francesch A 2023 Adaptive magnetoactive soft composites for modular and reconfigurable actuators *Adv. Funct. Mater.* **33** 2215248
- [32] Germann J, Dommer M, Pericet-Camara R and Floreano D 2012 Active connection mechanism for soft modular robots *Adv. Robot.* **26** 785–98
- [33] Marchese A D, Onal C D and Rus D 2011 Soft robot actuators using energy-efficient valves controlled by electropermanent magnets *2011 IEEE/RSJ Int. Conf. on Intelligent Robots and Systems* pp 756–61
- [34] Morin S A, Kwok S W, Lessing J, Ting J, Shepherd R F, Stokes A A and Whitesides G M 2014 Elastomeric tiles for the fabrication of inflatable structures *Adv. Funct. Mater.* **24** 5541–9
- [35] Ye Z, Lum G Z, Song S, Rich S and Sitti M 2016 Phase change of gallium enables highly reversible and switchable adhesion *Adv. Mater.* **28** 5088–92
- [36] Gomez E F, Wanasinghe S V, Flynn A E, Dodo O J, Sparks J L, Baldwin L A, Tabor C E, Durstock M F,

- Konkolewicz D and Thrasher C J 2021 3D-printed self-healing elastomers for modular soft robotics *ACS Appl. Mater. Interfaces* **13** 28870–7
- [37] Yang H, Jin S and Wang W D 2022 Modular assembly of soft machines via multidirectional reclosable fasteners *Adv. Intell. Syst.* **4** 2200048
- [38] McDonald K J, Kinnicutt L, Moran A M and Ranzani T 2022 Modulation of magnetorheological fluid flow in soft robots using electropermanent magnets *IEEE Robot. Autom. Lett.* **7** 3914–21
- [39] Craig R 2011 *Mechanics of Materials* (Wiley) (<https://doi.org/10.1016/j.mechmat.2010.12.004>)
- [40] Zou Y, Kim D, Norman P, Espinosa J, Wang J-C and Virk G S 2022 Towards robot modularity—a review of international modularity standardization for service robots *Robot. Autom. Syst.* **148** 103943
- [41] Fang Z, Fu Y and Chai T 2009 A low-cost modular robot for research and education of control systems, mechatronics and robotics 2009 4th IEEE Conf. on Industrial Electronics and Applications pp 2828–33